Finite-time tracking control of a nonlinear string to reference dynamics

Marc Wijnand[1], Thomas Hélie[2] and David Roze[2]
S3AM team, STMS Lab (IRCAM – [2]CNRS – [1]Sorbonne Université), Paris, France
marc.wijnand@ircam.fr

Summary. This paper is concerned with the active control of a string. A nonlinear Kirchhoff-Carrier model of the transverse vibration of a string is considered (presenting a pitch glide at high excitation levels), controlled by a force in its domain. A finite-time tracking controller is designed for a point force, that controls one mode of the string to reference dynamics corresponding to a string with other physical parameters. We illustrate in a simulation how the controller can be used to modify the damping, resonance frequency or the presence of a pitch glide for the selected mode of vibration of the string.
A preliminary version of this work has appeared in [1, Ch. 8].

Introduction

Active vibration control

In a lot of engineering applications, vibration is unwanted as it leads to negative side-effects such as increased wear of components or time and quality loss in production processes. Therefore, numerous *active vibration control* methods have been developed [2, 3], that aim at reducing parasitic vibration.
If a system representation based on the vibration modes is considered, the term *modal control* is used.

Active control of musical instruments

Active control of musical instruments consists in adding a control loop to an existing acoustic musical instrument that is being played by a musician. The terms *augmented* or *hybrid musical instruments* are also used. In some cases, communication to other devices is included, and the term *smart instruments* is used [4].
In terms of the actuator type, two classes of active vibration control are distinguished. In the case of *acoustical active control*, the control acts on a fluid medium. An example is the use of a loudspeaker to create destructive interference in order to cancel sound. In the case of *structural acoustical control*, the control acts on a solid. One can for example attach an actuator to the soundboard of a violin.
In most cases of active control of musical instruments, the goal is not to reduce vibrations as much as possible, but to change frequencies or damping coefficients of the instrument's vibration, enabling the musician to enlarge his sound palette while keeping the ergonomics of the original instrument. One can mention for instance applications to the (xylophone) beam [5], (clarinet) tube [6], (Chinese gong) metal plate [7] and (tom) membrane [8].
Furthermore, active control of musical instruments can be invoked for the study of their dynamical behaviour [9], or for the removal of unwanted phenomena such as the so-called wolf note of the cello [10], or the bad playability of certain notes on the trombone when using a straight mute [11].

Active control of a string

There exists a considerable amount of results concerning the vibration suppression of the string, both in the linear case and using models with different kinds of nonlinearities. The string can be actuated at its boundaries or in its domain, sometimes taking into account ODE dynamics of systems coupled to the string. A broad variety of control design methods have been used, that have been tested in simulation and experimentally.
In particular, tracking control has been used in [12, 13] where a boundary control to a string is designed that lets a mass attached to it follow a reference position. In applications involving axially moving strings, axial velocity tracking has also been used [14].

Active control of a musical string

In a musical context, the goal of active control is to influence the vibration of strings present in violins, pianos, guitars, etc. and that are made of a variety of materials such as nylon and metal. Used string displacement sensors can be electromagnetic [15], piezoelectric [16] or optical (for example [17, 18]). As string actuator, one can use an electromagnetic actuation (for example with the commercially available *EBow* [19] or the alternative [20] in the case of metal strings, or the use of a magnet attached to a nonmagnetic string [17]), or a piezoelectric actuator [21].
Concerning the control of an isolated string, following results have been reported. In [22], the principles of a PID control of a string are discussed, using a collocated sensor and actuator, and enabling to modify resonance frequency and damping. Furthermore, several experimental setups for string control have been considered. In [23], a metal guitar string of length 24 cm tuned to 248 Hz was damped using an optical sensor and an electromagnetic actuator [20]. In [24], the first five modes of a guitar string were damped using a feedback measuring string displacement with a laser, and an electromagnetic actuation. In [21], the setup consisted of a metal guitar string of 50 cm tuned to 220 Hz, an optical string displacement sensor and a piezoelectric actuator at one end of the string. Based on traveling wave control concepts, active damping is achieved, and nonlinearities can be injected, leading to timbral effects.
Active control of other instrument parts coupled to the vibrating string is also possible, such as the violin bridge [25] and the soundboard of a monochord, acoustical guitar and cello [26]. In [27], the construction of a piano with active control is reported, with a piezoelectric sensor on the soundboard and electromagnets over the 88 sets of strings actuators. It is

possible to generate infinite sustain, crescendo on a note and different timbral effects. Finally, an embedded control system using multiple sensors and actuators can be found in some commercially available instruments such as the *Sensus Smart Guitar* (MIND Music Labs, [4]) and the *Smart Acoustic Guitar* (HyVibe, [28]).

Aim and structure of the present paper

This contribution is concerned with the control of a selected mode of the nonlinear Kirchhoff-Carrier string model by a point force for which a finite-time tracking control law is developed. First, the nonlinear string model is recalled, recast as a Port-Hamiltonian System, and projected on the modes of the linearized system. Next, the finite-time tracking controller for a chosen mode is developed, enabling to track a reference trajectory representing a mode with modified physical parameters. Finally, the effect of the control law is illustrated by a simulation.

Nonlinear string model

The Kirchhoff-Carrier string model is recalled. This PDE is subsequently recast as a Port-Hamiltonian system, to which an order reduction by modal projection and truncation is applied. Thus, each mode is represented by a coupled nonlinear ODE.

PDE model

The nonlinear Kirchhoff-Carrier model for the transverse vibrations $w(z,t)$ [m] of a string of length L [m] is considered [29, 30]:

$$\rho A \partial_{tt} w(z,t) + \rho A \mu \partial_t w(z,t) - \left(T_0 + \frac{EA}{2L} \int_\Omega \left(\partial_z w(z,t)\right)^2 \, \mathrm{d}z \right) \partial_{zz} w(z,t) = \frac{1}{L} u(z,t), \tag{1}$$

with ρ [kg/m^3] the mass density, A [m^2] the circular cross-section, μ [1/s] a positive coefficient representing viscous damping (see [31, §5.3.2]), T_0 [N] the tension, E [Pa] Young's modulus of elasticity and $u(z,t)$ [N] the distributed exciting force defined on $(z,t) \in \Omega \times \mathbb{R}^+$, $\Omega = [0, L]$. The nonlinearity is due to the variation of tension expressed by the integral term $\frac{EA}{2L} \int_\Omega \left(\partial_z w(z,t)\right)^2 \, \mathrm{d}z$ (with $EA \gg T_0$, [32, Ch. 8]), leading to the pitch-glide phenomenon (illustrated in the *Simulation* Section). The string is fixed at its ends (Dirichlet boundary condition) and initially at rest:

$$\begin{aligned} &w(z=0,t) = 0 && w(z=L,t) = 0 && \forall t \in \mathbb{R}^+ \\ &w(z,t=0) = 0 && w(z,t=0) = 0 && \forall z \in \Omega. \end{aligned}$$

This setup is depicted in Fig. 1.

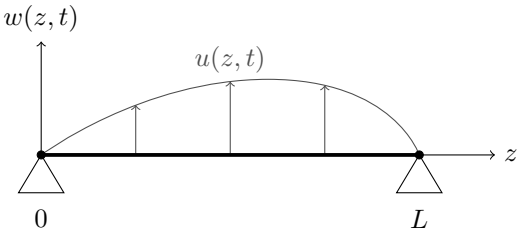

Figure 1: Setup of the PDE model for a string that is initially at rest ($w(z,t) = 0$) and subjected to a distributed force $u(z,t)$

Port-Hamiltonian system model

Components of an open physical system can (1) exchange energy inside the system; (2) dissipate energy; (3) exchange energy with the exterior of the system through ports. The power balance of the system is satisfied at all time. This is taken into account in the Port-Hamiltonian framework [33].

An infinite-dimensional Port-Hamiltonian system (PHS) can be defined as [34, 35]

$$\begin{cases} \partial_t \boldsymbol{x} = (\mathcal{J} - \mathcal{R}) \delta_{\boldsymbol{x}} \mathcal{H}(\boldsymbol{x}) + \mathcal{G} \boldsymbol{u} \\ \quad \boldsymbol{y} = \mathcal{G}^\star \delta_{\boldsymbol{x}} \mathcal{H}(\boldsymbol{x}), \end{cases}$$

where

- the state $\boldsymbol{x}$ belongs to the energy state space $\mathbb{X}$;
- a scalar product $\langle \cdot, \cdot \rangle_{\mathbb{X}}$ and norm $\|\cdot\|_{\mathbb{X}}$ are defined;
- the Hamiltonian function is defined as $\mathcal{H}(\boldsymbol{x}) \triangleq \frac{1}{2} \|\boldsymbol{x}\|_{\mathbb{X}}^2$;
- the operator $\delta_{\boldsymbol{x}}$ is the variational derivative [35];

- the interconnection operator $\mathcal{J}$ is formally skew-symmetric and the dissipation operator $\mathcal{R}$ is non-negative symmetric, w.r.t. the scalar product;
- the product of the input $\boldsymbol{u}$ and its associated output $\boldsymbol{y}$ represents the power applied to the system via the ports;
- $\mathcal{G}^*$ represents the adjoint operator of the operator $\mathcal{G}$.

In the finite-dimensional case ($\boldsymbol{x} \in \mathbb{R}^n$), the operators become matrices and $\delta_{\boldsymbol{x}}$ is replaced by the gradient $\boldsymbol{\nabla}_{\boldsymbol{x}}$ [33]. We refer the reader to [36, 37] where the example of a (non)linear mass-spring-damper system is treated.
Next to modeling physical systems, the PHS formalism provides a framework for the development of stable simulation [38] and control [39] methods.

Port-Hamiltonian string model
As shown in [40], the nonlinear string (1) can be recast as an infinite-dimensional Port-Hamiltonian System with state $\boldsymbol{x}^T(z,t) \triangleq \begin{bmatrix} q(z,t) & p(z,t) \end{bmatrix} \triangleq \begin{bmatrix} \partial_z w(z,t) & \partial_t w(z,t) \end{bmatrix}$, and nonquadratic Hamiltonian function [32, Ch. 8]

$$\mathcal{H}(\boldsymbol{x}(z,t)) = \frac{\rho A}{2} \int_\Omega p^2(z,t)\,\mathrm{d}z + \frac{1}{2}\left[T_0 + \frac{EA}{4L}\int_\Omega q^2(z,t)\,\mathrm{d}z\right]\int_\Omega q^2(z,t)\,\mathrm{d}z, \tag{2}$$

leading to the following infinite-dimensional PHS formulation:

$$\begin{cases} \dfrac{\mathrm{d}}{\mathrm{d}t}\begin{bmatrix} q \\ p \end{bmatrix} = \left(\begin{bmatrix} 0 & \frac{1}{\rho A}\partial_z \\ \frac{1}{\rho A}\partial_z & 0 \end{bmatrix} - \begin{bmatrix} 0 & 0 \\ 0 & \frac{1}{\rho A}\mu \end{bmatrix}\right)\begin{bmatrix} \delta_q \mathcal{H} \\ \delta_p \mathcal{H} \end{bmatrix} + \begin{bmatrix} 0 \\ \frac{1}{\rho A L} \end{bmatrix} u \\ \qquad y = \begin{bmatrix} 0 & \frac{1}{\rho A L} \end{bmatrix}\begin{bmatrix} \delta_q \mathcal{H} \\ \delta_p \mathcal{H} \end{bmatrix}, \end{cases} \tag{3}$$

with the variational derivative of the Hamiltonian function (2) equal to

$$\delta_{\boldsymbol{x}}\mathcal{H}(\boldsymbol{x}(z,t)) = \begin{bmatrix} \delta_q \mathcal{H}(\boldsymbol{x}(z,t)) \\ \delta_p \mathcal{H}(\boldsymbol{x}(z,t)) \end{bmatrix} = \begin{bmatrix} \left(T_0 + \frac{EA}{2L}\int_0^L q^2(z,t)\,\mathrm{d}z\right) q(z,t) \\ \rho A\, p(z,t) \end{bmatrix}.$$

The input $u(z,t)$ being the force applied to the string, and the output $y(z,t) = (1/L)\partial_t w(z,t)$ with $\partial_t w(z,t)$ the transverse velocity, the expression $\int_\Omega u(z,t)y(z,t)\,\mathrm{d}z$ [W] represents the instantaneous external power transferred to the string.

Modal projection and order reduction
The infinite-dimensional PHS model (3) is projected on the N first eigenmodes of the linear string (Eq. (1) without the term $\frac{EA}{2L}\int_\Omega (\partial_z w(z,t))^2\,\mathrm{d}z$), that are given by $e_n(z) = \sqrt{\frac{2}{L}}\sin\left(\frac{n\pi}{L}z\right), n > 0$ (Fig. 2):

$$w(z,t) \approx \sum_{n=1}^{N} e_n(z) W_n(t).$$

Figure 2: First 6 eigenmodes $e_n(z)$ of the linear string of length L. The nodes (stationary points) are indicated by dots.

Then, defining

$$\boldsymbol{x}(z,t) = \begin{bmatrix} \frac{\mathrm{d}}{\mathrm{d}z}e_1(z) \dots \frac{\mathrm{d}}{\mathrm{d}z}e_N(z) & \boldsymbol{O}_{1\times N} \\ \boldsymbol{O}_{1\times N} & e_1(z)\dots e_N(z) \end{bmatrix}\begin{bmatrix} \boldsymbol{W}(t) \\ \frac{\mathrm{d}}{\mathrm{d}t}\boldsymbol{W}(t) \end{bmatrix} = \boldsymbol{\Phi}^\intercal(z)\boldsymbol{X}(t), \tag{4}$$

the Hamiltonian function $\mathcal{H}(\boldsymbol{x}(z,t)) = \frac{1}{2}\int_0^1 \boldsymbol{x}^\intercal(z,t)\mathcal{M}(z,t)\boldsymbol{x}(z,t)\,\mathrm{d}z$ (2) becomes

$$H(\boldsymbol{X}(t)) = \frac{1}{2}\int_0^1 \boldsymbol{X}^\intercal(t)\boldsymbol{\Phi}(z)\mathcal{M}(z,t)\boldsymbol{\Phi}^\intercal(z)\boldsymbol{X}(t)\,\mathrm{d}z = \frac{1}{2}\boldsymbol{X}^\intercal(t)\boldsymbol{M}_N(t)\boldsymbol{X}(t),$$

with

$$\boldsymbol{M}_N(t) = \begin{bmatrix} \boldsymbol{D}_N^2\left(T_0 + \frac{EA}{4L}\boldsymbol{X}^\intercal(t)\boldsymbol{N}_N\boldsymbol{X}(t)\right) & \boldsymbol{O}_{N\times N} \\ \boldsymbol{O}_{N\times N} & \rho A\boldsymbol{I}_{N\times N} \end{bmatrix}, \quad \boldsymbol{N}_N = \begin{bmatrix} \boldsymbol{D}_N^2 & \boldsymbol{O}_{N\times N} \\ \boldsymbol{O}_{N\times N} & \boldsymbol{O}_{N\times N} \end{bmatrix}, \quad \boldsymbol{D}_N^2 = \frac{\pi^2}{L^2}\mathrm{diag}(1, 2^2, \dots, N^2).$$

Next, premultiplying the first equation of the PHS (3) by $\boldsymbol{\Phi}(z)$, integrating it w.r.t. $z \in \Omega$, substituting (4) and using the localized controller setup (7) that will be defined below, one obtains following finite-dimensional PHS:

$$\begin{cases} \dfrac{\mathrm{d}}{\mathrm{d}t}\boldsymbol{X}(t) = \left(\dfrac{1}{\rho A}\begin{bmatrix} \boldsymbol{O}_{N\times N} & \boldsymbol{I}_{N\times N} \\ -\boldsymbol{I}_{N\times N} & \boldsymbol{O}_{N\times N} \end{bmatrix} - \dfrac{\mu}{\rho A}\begin{bmatrix} \boldsymbol{O}_{N\times N} & \boldsymbol{O}_{N\times N} \\ \boldsymbol{O}_{N\times N} & \boldsymbol{I}_{N\times N} \end{bmatrix}\right) \begin{bmatrix} \boldsymbol{D}_N^2(T_0 + \frac{EA}{2L}\boldsymbol{X}^\intercal(t)\boldsymbol{N}_N\boldsymbol{X}(t)) & \boldsymbol{O}_{N\times N} \\ \boldsymbol{O}_{N\times N} & \rho A\boldsymbol{I}_{N\times N} \end{bmatrix} \boldsymbol{X}(t) \\ \qquad\qquad + \dfrac{1}{\rho AL}\begin{bmatrix} \boldsymbol{O}_{N\times 1} \\ \varphi_1 \\ \vdots \\ \varphi_N \end{bmatrix} U(t) \\ y(z,t) = \begin{bmatrix} 0 & \frac{1}{L} \end{bmatrix} \boldsymbol{\Phi}^\intercal(z)\boldsymbol{X}(t), \end{cases} \tag{5}$$

with $\varphi_n \triangleq e_n(\ell)$, and ℓ and $U(t)$ will be defined by (7).
The $(N+n)^{\text{th}}$ line of the dynamics for $\boldsymbol{X}(t)$ gives

$$\ddot{W}_n(t) = -\frac{1}{\rho A}n^2\frac{\pi^2}{L^2}\left(T_0 + \frac{EA}{2L}\Sigma(t)\right)W_n(t) - \mu\dot{W}_n(t) + \frac{\varphi_n}{\rho AL}U(t), \tag{6}$$

where

$$\Sigma(t) \triangleq \sum_{n=1}^{N} n^2\frac{\pi^2}{L^2}W_n^2(t).$$

Each mode n is a nonlinear oscillator with a coupling to the other modes due to the term $\Sigma(t)$, and that is controlled by $U(t)$.

Finite-time tracking control

Hypotheses concerning the control layout are made and the control goal is stated. Then, an existing finite-time control law is applied to obtain the tracking controller that will control one mode of the nonlinear string (5) to chosen reference dynamics.

Controller setup

Following hypotheses are made.

1. *(Point force)* We use a single actuator that is able to deliver a localized force $U(t)$ [N]:

   $$u(z,t) \triangleq \delta(z-\ell)U(t), \tag{7}$$

   with $\delta(z-\ell)$ the Dirac delta distribution that activates the control law $U(t)$ at the position $z=\ell$ (cf. Fig. 3).

   Furthermore, we suppose here that the application of a force at $z=\ell$ does not modify the eigenmodes $e_n(z)$. Then, one can write

   $$u(z,t) = \sum_{n=1}^{N}\langle u(z,t), e_n(z)\rangle \cdot e_n(z) = \sum_{n=1}^{N} e_n(\ell)U(t)\cdot e_n(z) \triangleq \sum_{n=1}^{N}\varphi_n U(t)\cdot e_n(z).$$

   Because of this hypothesis, the force $\varphi_n U(t)$ is applied to each mode n. Therefore, only one mode can be controlled at a time.

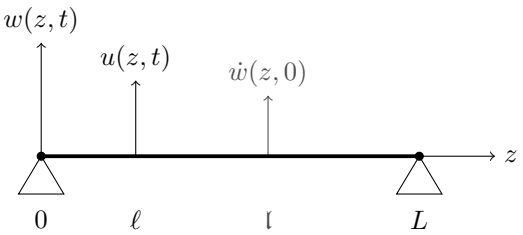

Figure 3: String that is initially at rest, subjected to a point force at $z=\ell$, and with an initial velocity applied at $z=\iota$ (see *Simulation*)

2. *(Known state)* It is supposed that the entire state $\boldsymbol{X}(t)$ of the projected PHS model (5) is known from the measured system output[1] $\boldsymbol{y}_{\text{meas}}(z,t)$, possibly after using an observer.

[1] In general, the measured output $\boldsymbol{y}_{\text{meas}}(z,t)$ differs from the PHS output $\boldsymbol{y}(z,t)$ defined as the conjugated variables with respect to the system input variables $\boldsymbol{u}(z,t)$, in the sense that $\int_\Omega \boldsymbol{u}(z,t)\boldsymbol{y}(z,t)\,\mathrm{d}z$ represents the instantaneous power applied to the PHS.

Control goal

A system $\{\mathcal{S}\}$ described by (5) represents the dynamics of the first N modes of the nonlinear string with physical parameters (ρ, T_0, μ, E). Following Hypothesis 1, our goal is to construct a controller $\{\mathcal{C}\}$ that lets one mode of the real system $\{\mathcal{S}\}$ track the dynamics of a virtual reference system $\{\mathcal{S}^*\}$ with desired physical parameters $(\rho^*, T_0^*, \mu^*, E^*)$, for an excitation by the same initial conditions (Fig. 4). To this means, a finite-time tracking controller will be designed.

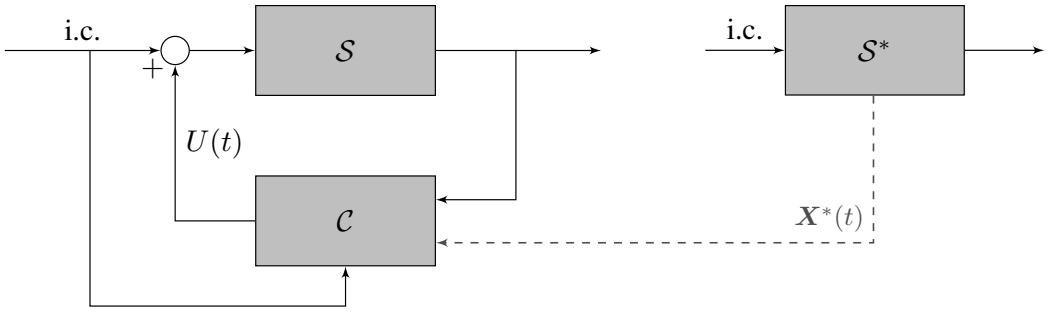

(a) Closed loop system $\{\mathcal{S}\&\mathcal{C}\}$ (b) Desired system dynamics $\{\mathcal{S}^*\}$

Figure 4: Tracking control layout (i.c.: initial conditions). The dashed arrow represents the reference trajectory $\boldsymbol{X}^*(t)$ corresponding to the reference system $\{\mathcal{S}^*\}$ that is in reality simulated inside the controller $\{\mathcal{C}\}$.

Finite-time control

Finite-time control [41] is a nonlinear control method enabling to reach an equilibrium point in a finite time. This finite settling time is a stronger property than in the case of asymptotic or exponential control. Finite-time control has useful properties for time-constraint and robust control [42].
Finite-time stability of an ODE with state $\boldsymbol{x}(t) \in \mathbb{R}^n$ is defined as follows.

Definition 1 (Finite-time stability [42]) *Let $\dot{\boldsymbol{x}} = \boldsymbol{F}(\boldsymbol{x})$ represent a closed-loop system, with $\boldsymbol{F}(\boldsymbol{x})$ continuous and $\boldsymbol{F}(\boldsymbol{0}) = \boldsymbol{0}$. Let $\boldsymbol{\Psi}^t(\boldsymbol{x}_0)$ be the time evolution of the state for a given initial state $\boldsymbol{x}_0$.*
The origin is a finite-time stable *equilibrium if there exists an open neighborhood $U \subset \mathbb{R}^n$ of the origin, where following statements hold:*

1. ***Finite-time convergence.** There exists a settling-time function $T : U\backslash\{0\} \to \mathbb{R}_{\geq 0}$ such that for each $\boldsymbol{x}_0 \in U\backslash\{0\}$, the evolution $\boldsymbol{\Psi}^t(\boldsymbol{x}_0)$ is defined and unique on $t \in [0, T(\boldsymbol{x}_0)[$ and $\lim_{t \to T(\boldsymbol{x}_0)} \boldsymbol{\Psi}^t(\boldsymbol{x}_0) = 0$.*
2. ***Lyapunov stability.** There exists a monotonically increasing function $\delta(\cdot)$, $\delta(0) = 0$, such that for each $\boldsymbol{x}_0 \in U$, $\|\boldsymbol{\Psi}^t(\boldsymbol{x}_0)\| \leq \delta(\|\boldsymbol{x}_0\|)$ for each $t \geq 0$.*

Furthermore, if $U = \mathbb{R}^n$, the origin is globally finite-time stable.

Several finite-time control laws have been designed for different kinds of ODE systems. They necessarily are non Lipschitz continuous at the equilibrium point [41]. For ODE systems of dimension $n = 2$, following law can be used.

Lemma 1 (Finite-time stabilisation of the double integrator [43]) *The origin of the double integrator*

$$\begin{cases} \dot{z}_1(t) = z_2(t) \\ \dot{z}_2(t) = v(t) \end{cases} \tag{8}$$

is finite-time stable for the control law

$$v(t) = -\kappa_1 \lfloor z_1(t) \rceil^{\frac{\alpha}{2-\alpha}} - \kappa_2 \lfloor z_2(t) \rceil^{\alpha},$$

where $\kappa_1, \kappa_2 > 0$, $\alpha \in]0, 1[$ and $\lfloor z \rceil^{\alpha} \triangleq \operatorname{sign}(x)|x|^{\alpha}$.

No explicit expression for the dependence of the settling-time on the control parameters $(\kappa_1, \kappa_2, \alpha)$ is known. Therefore, these parameters have to be tuned numerically. We refer the reader to [37] for an application of this law to a (non)linear mass-spring-damper system.

Finite-time tracking control applied to the nonlinear string

A finite-time tracking controller is developed for a chosen mode $M \in [\![1, \ldots, N]\!]$ by imposing the dynamics of (8) to the error

$$e(t) \triangleq W_M(t) - W_M^*(t)$$

between the real modal displacement $W_M(t)$ and the reference modal displacement $W_M^*(t)$ of mode M. A finite-time stabilization of

$$W_M(t) \to W_M^*(t), \quad \dot{W}_M(t) \to \dot{W}_M^*(t)$$

is thus obtained for the error dynamics

$$\frac{\mathrm{d}}{\mathrm{d}t}\begin{bmatrix} e(t) \\ \dot{e}(t) \end{bmatrix} = \begin{bmatrix} \dot{e}(t) \\ -\kappa_1 \lfloor e(t) \rceil^{\frac{\alpha}{2-\alpha}} - \kappa_2 \lfloor \dot{e}(t) \rceil^{\alpha} \end{bmatrix}. \tag{9}$$

After substituting the expression (6) for the real ($W_M(t)$) and desired ($W_M^*(t)$) oscillators, one solves (9) for the control law $U(t)$, which corresponds to

$$\begin{aligned} U(t) = \frac{1}{\varphi_M}\Bigg[& -\rho A L \left(\kappa_1 \lfloor W_M - W_M^* \rceil^{\frac{\alpha}{2-\alpha}} + \kappa_2 \left\lfloor \dot{W}_M - \dot{W}_M^* \right\rceil^{\alpha} \right) \\ & + M^2 \frac{\pi^2}{L} \left(T_0 W_M - \frac{\rho}{\rho^*} T_0^* W_M^* + \frac{A}{2L} \left(E\Sigma W_M - \frac{\rho}{\rho^*} E^* \Sigma^* W_M^* \right) \right) + \rho A L \left(\mu \dot{W}_M - \mu^* \dot{W}_M^* \right) \Bigg]. \end{aligned} \tag{10}$$

Applying this finite-time tracking control law to the system $\mathcal{S}$ will control its M^{th} mode to the M^{th} mode of the reference system $\mathcal{S}^\star$. As previously mentioned, because of Hypothesis 1, we do not have additional degrees of freedom to act on the other modes $n \neq M$.
The design of the control parameters $(\kappa_1, \kappa_2 > 0, \alpha \in]0,1[)$ present in the tracking controller has to ensure that it has faster dynamics than the dynamics of the nonlinear string (by Tikhonov's theorem, see for instance [44, Theorem A.11]). Their values have to be assessed by a simulation, that is presented in the next session.

Simulation

A system $\{\mathcal{S}\}$ is considered, with physical parameters from [45, Table 1] representing a steel string with fundamental frequency $f = \frac{1}{2L}\sqrt{\frac{T_0}{\rho A}} = 55\,\text{Hz}$:

$$L = 1{,}8\,\text{m}, \qquad A = \pi \cdot (1{,}5\,\text{mm})^2, \qquad \rho = 7800\,\frac{\text{kg}}{\text{m}^3}, \qquad E = 2 \cdot 10^{11}\,\text{Pa}, \qquad \mu = 3\,\frac{1}{\text{s}}, \qquad T_0 = 2161\,\text{N}.$$

The string is excited by an initial velocity localized at $z = \mathfrak{l}$ (Fig. 3):

$$\dot{w}(z,0) = V_0 \left[\frac{\text{m}}{\text{s}}\right] \cdot \delta(z - \mathfrak{l}),$$

whose projection on mode $e_n(z)$ yields the initial conditions $\dot{W}_n(0) = V_0\sqrt{\frac{2}{L}}\sin\left(\frac{n\pi}{L}\mathfrak{l}\right)$, $n \in [\![1, \ldots, N]\!]$.
The controlled system $\{\mathcal{S}\&\mathcal{C}\}$ using control law (10) is simulated for two cases:

① a reference system $\{\mathcal{S}^*\}$ where the parameters (T_0, ρ, μ) of the linearized string model are modified for the mode $M = 2$, leading to a change in frequency and damping,

② a reference system $\{\mathcal{S}^*\}$ where the parameter E of the nonlinear string model is modified for the mode $M = 1$, leading to a modification of the pitch-glide effect.

The simulations are performed using the backwards Euler method [46] with time step $\delta t = 10^{-5}\,\text{s}$, using $N = 10$ modes and initial conditions with $V_0 = 50\,\frac{\text{m}}{\text{s}}$. Excitation location $\mathfrak{l}$ and control location ℓ will be set in function of the shape of the chosen controlled mode M (cf. Fig. 2, and [22, §II.C]).

Example ①: frequency and damping modification

Modifying the tension T_0 and/or mass density ρ, one can change the frequency of the M^{th} mode: $f_M^* = \frac{M}{2L}\sqrt{\frac{T_0^*}{\rho^* A}}$, whereas modifying the damping coefficient μ enables to damp the string quicker (active damping) or less quick (infinite sustain).
We consider the case where the string is excited at $\mathfrak{l} = \frac{1}{4}L$ and controlled at $\ell = \frac{3}{4}L$. The mode $M = 2$ is controlled to a reference trajectory with $T_0^* = 1.12T_0$ and $\rho^* = 0.88\rho$ (corresponding to $f_2^* = 124$ Hz $> f_2 = 110$ Hz), $\mu^* = 1.5\mu$ (increased damping), $E^* = E$ (no pitch-glide modification). Control parameters $\kappa_i = 0.5 \cdot 10^{11}$ and $\alpha = 0.95$ were used.
A tracking of the reference signal $W_2^*(t)$ is achieved by $W_2(t)$ under the action of the control law $U(t)$ (Fig. 5). The spectral content of the second mode (Fig. 7) confirms that its frequency was increased to f_2^*, and that the signal is damped more quickly.
One can observe the effects of the control law $U(t)$ on the other modes $n \neq 2$, such as the appearance of low-amplitude harmonics in the higher-order modes, that cannot be influenced in the current control setup. Furthermore, we note that the 4^{th} mode is not excited by the initial conditions nor by the control law $U(t)$, as both are located at a node of this mode ($\dot{W}_4(0) = 0, \varphi_4 = 0$; cf. Fig. 2).

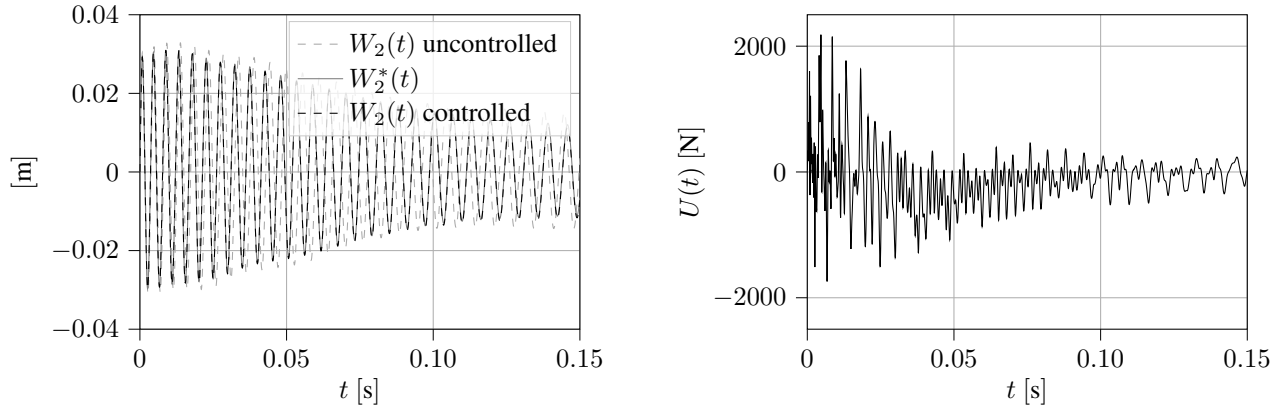

(a) Controlled mode 2

(b) Control law

Figure 5: Example ①: controlled mode 2 and control law

Example ②: pitch-glide attenuation

A pitch glide is the nonlinear phenomenon where the frequency increases with increasing amplitude of the transverse vibration $w(z,t)$ of the string, because of the tension modulation expressed by the term

$$\frac{EA}{2L}\int_\Omega (\partial_z w(z,t))^2 \,\mathrm{d}z$$

in (1). This phenomenon was visible in Example ① (Fig. 7).

In this second example, we consider the case where the string is excited at $\mathfrak{l} = 0.4L$ and controlled at $\ell = 0.5L$. The mode $M = 1$ is controlled to a reference trajectory with $T_0^* = T_0$ and $\rho^* = \rho$ (no frequency modification), $\mu^* = \mu$ (no damping modification) and $E^* = 0.3E$ (pitch-glide attenuation[2]). Control parameters $\kappa_i = 1 \cdot 10^{10}$ and $\alpha = 0.95$ were used.

A tracking of the reference signal $W_1^*(t)$ is achieved by $W_1(t)$ under the action of the control law $U(t)$ (Fig. 6). The spectral content of the first mode (Fig. 8) confirms that the pitch-glide phenomenon is attenuated.

Again, one can observe the effects of the control law $U(t)$ on the other modes $n \neq 1$, that cannot be influenced in the current control setup. In particular, the pitch-glide effect is increased for the second mode (and higher modes, although their amplitude is smaller), and harmonics appear in the higher-order modes.

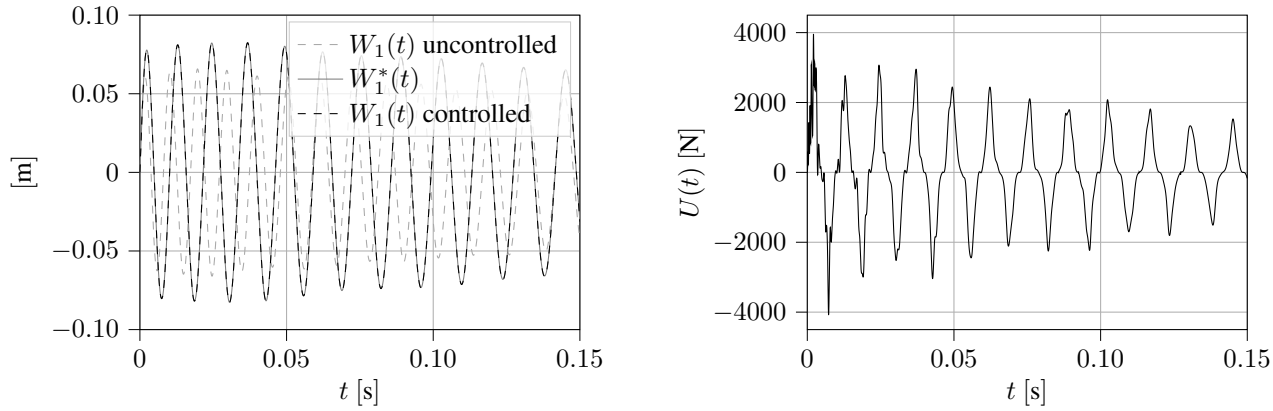

(a) Controlled mode 1

(b) Control law

Figure 6: Example ②: controlled mode 1 and control law

Conclusions and perspectives

A tracking controller was designed, that is able to modify physical model parameters of a chosen mode of a truncated modal model of a nonlinear Kirchhoff-Carrier string taking into account the pitch-glide phenomenon. Two use cases were illustrated in simulation, where frequency, damping and the pitch glide-phenomenon were modified, and the effect on the other modes was observed.

Future works include the consideration of a more realistic sensor and actuator setup taking into account their placement [22, §II.C] and the development of an observer in order to reconstruct the state. Furthermore, robustness of the controller against measurement noise or bad parameter estimation can be assessed.

[2] A reference stiffness of $E^* = 0$ would correspond to a pitch-glide removal, but requires unrealistic force levels of 30 kN for $U(t)$. This control goal was used in the preliminary simulation shown in [1, §8.4]. An analysis of the required control power as in [22, Appendix B] is not performed here.

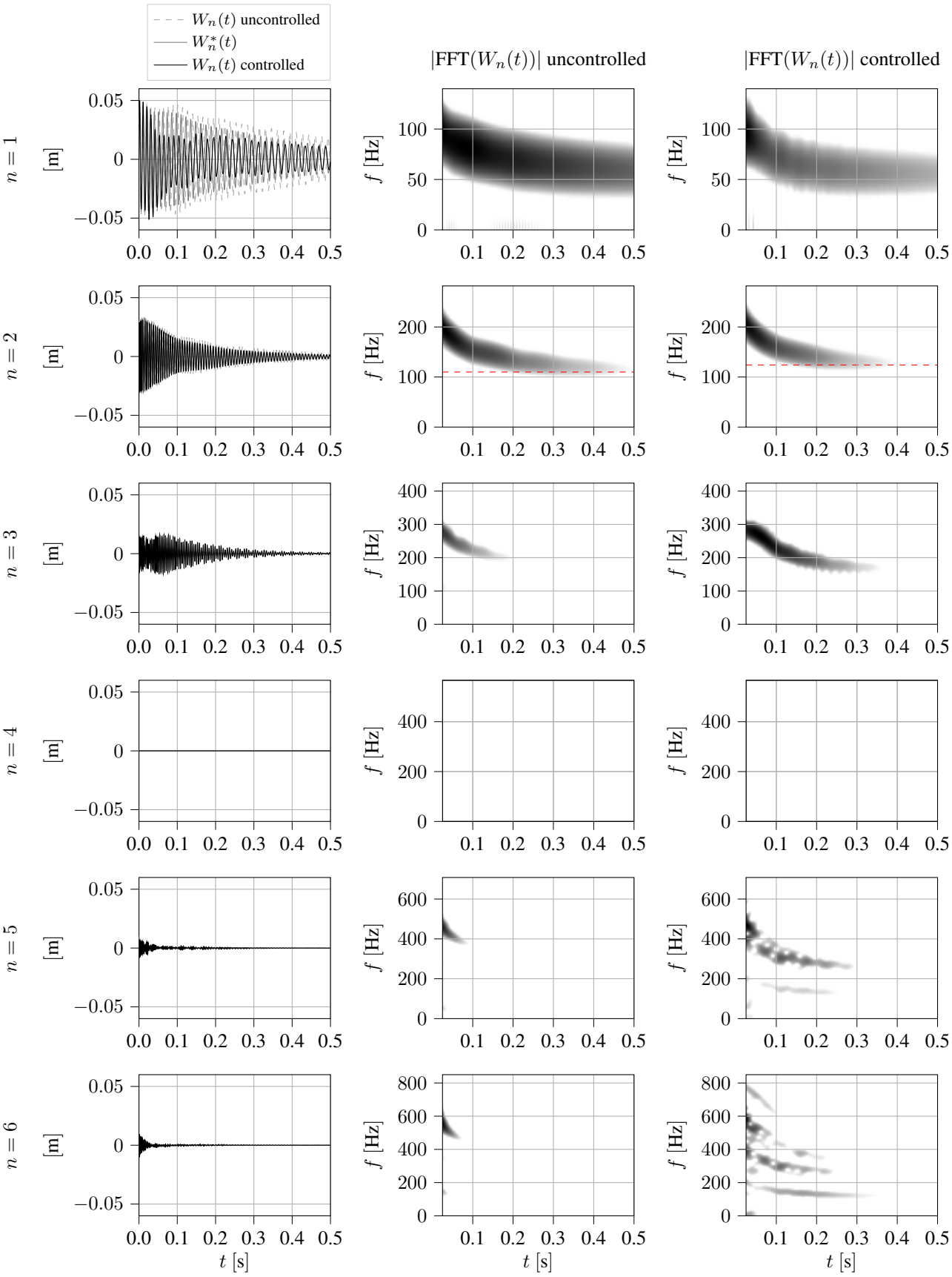

Figure 7: Example ①: time evolution and spectral content of the first 6 modes. The FFT is calculated using a Hann window and the same logarithmic color scale is used for the (un)controlled cases of a given mode. Red dashed lines indicate the asymptotic values of the frequencies (corresponding to the linearized string model) for mode 2 in the (un)controlled cases.

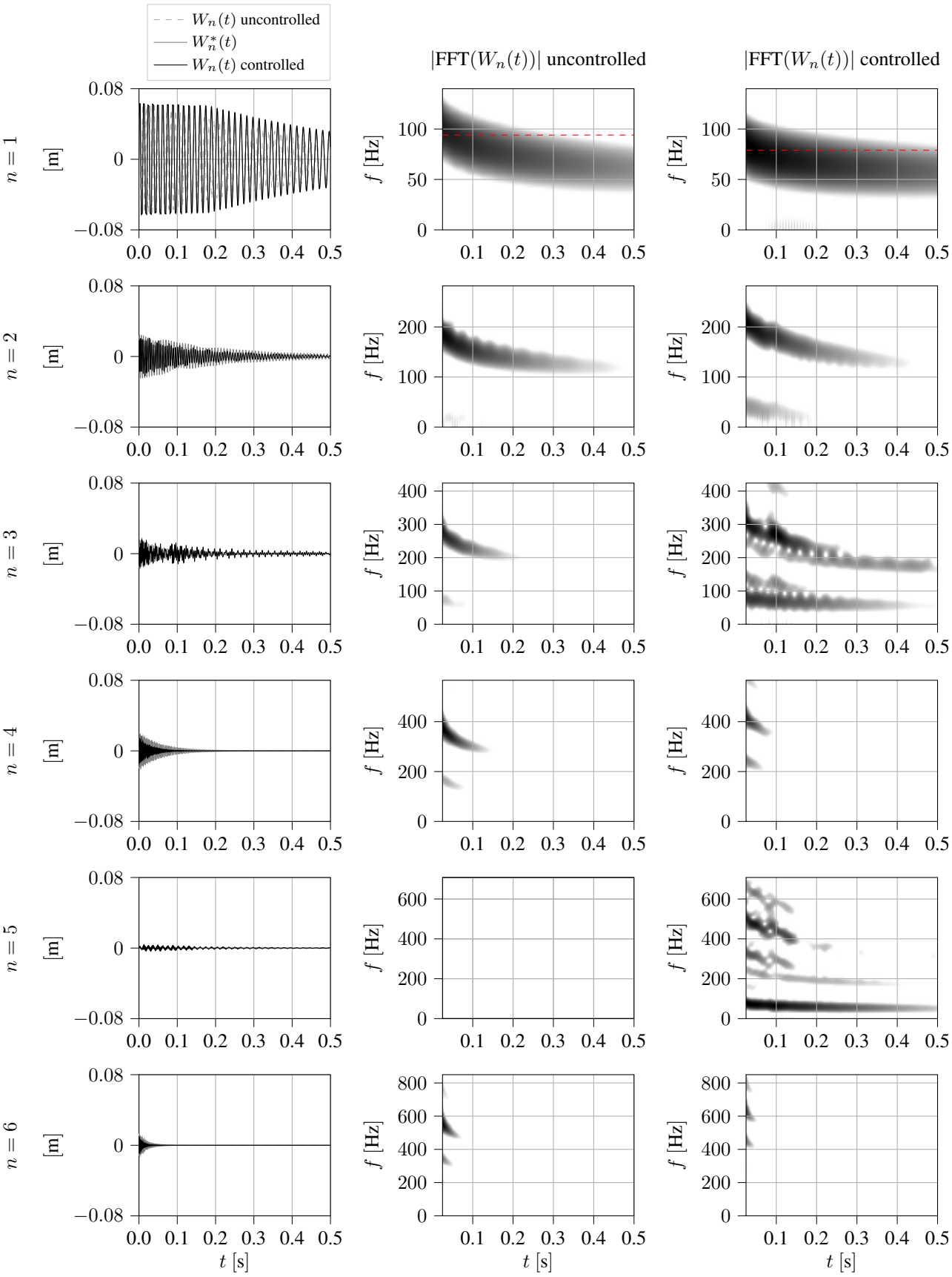

Figure 8: Example ②: time evolution and spectral content of the first 6 modes. The FFT is calculated using a Hann window and the same logarithmic color scale is used for the (un)controlled cases of a given mode. Red dashed lines indicate the starting frequencies of the pitch glide for mode 1 in the (un)controlled cases.

Acknowledgments

The authors thank the support of ANR project Finite4SoS (ANR 15 CE23 0007) and ANR-DFG project Infidhem (ANR 16 CE92 0028).

References

[1] Wijnand, M. (2021). *Contrôle en temps fini de systèmes vibratoires hybrides couplant équations aux dérivées partielles et équations aux dérivées ordinaires : les cas du tom et du câble pesant*. PhD thesis, Sorbonne Université, Paris, France.

[2] Elliott, S. J. and Nelson, P. A. (1993). Active noise control. *IEEE signal processing magazine*, 10(4):12–35.

[3] Fuller, C. C., Elliott, S., and Nelson, P. A. (1996). *Active control of vibration*. Academic Press.

[4] Turchet, L., McPherson, A., and Fischione, C. (2016). Smart instruments: towards an ecosystem of interoperable devices connecting performers and audiences. In *Proceedings of the Sound and Music Computing Conference*, pages 498–505.

[5] Boutin, H., Besnainou, C., and Polack, J.-D. (2015). Modifying the resonances of a xylophone bar using active control. *Acta Acustica united with Acustica*, 101(2):408–420.

[6] Meurisse, T., Mamou-Mani, A., Benacchio, S., Chomette, B., Finel, V., Sharp, D. B., and Caussé, R. (2015). Experimental Demonstration of the Modification of the Resonances of a Simplified Self-Sustained Wind Instrument Through Modal Active Control. *Acta Acustica united with Acustica*, 101(3):581–593.

[7] Jossic, M., Mamou-Mani, A., Chomette, B., Roze, D., Ollivier, F., and Josserand, C. (2017). Modal active control of Chinese gongs. *The Journal of the Acoustical Society of America*, 141(6):4567–4578.

[8] Wijnand, M., d'Andréa-Novel, B., Hélie, T., and Roze, D. (2020). Active control of the axisymmetric vibration modes of a tom-tom drum using a modal-based observer-regulator. In *EAA e-Forum Acusticum*.

[9] Benacchio, S., Mamou-Mani, A., Chomette, B., and Finel, V. (2016). Active control and sound synthesis–two different ways to investigate the influence of the modal parameters of a guitar on its sound. *The Journal of the Acoustical Society of America*, 139(3):1411–1419.

[10] Neubauer, P., Tschesche, J., Bös, J., Melz, T., and Hanselka, H. (2018). An active-system approach for eliminating the wolf note on a cello. *The Journal of the Acoustical Society of America*, 143(5):2965–2974.

[11] Meurisse, T., Mamou-Mani, A., Caussé, R., Sluchin, B., and Sharp, D. B. (2015). An active mute for the trombone. *The Journal of the Acoustical Society of America*, 138(6):3539–3548.

[12] Mounier, H., Rudolph, J., Fliess, M., and Rouchon, P. (1998). Tracking control of a vibrating string with an interior mass viewed as delay system. *ESAIM: Control, Optimisation and Calculus of Variations*, 3:315–321.

[13] Rudolph, J. and Woittennek, F. (2010). Flatness-based control without prediction: example of a vibrating string. *PAMM*, 10(1):629–630.

[14] Zhang, F., Nagarkatti, S. P., Costic, B., Dawson, D. M., and Rahn, C. D. (1999). Velocity Tracking Control of an Axially Accelerating String and Actuator System. In *Proceedings of the 38th IEEE Conference on Decision and Control (Cat. No. 99CH36304)*, volume 5, pages 4325–4330. IEEE.

[15] Paiva, R. C., Pakarinen, J., and Välimäki, V. (2012). Acoustics and modeling of pickups. *Journal of the Audio Engineering Society*, 60(10):768–782.

[16] Freed, A. and Isvan, O. (2000). Musical Applications of New, Multi-axis Guitar String Sensors. In *26th International Computer Music Conference*.

[17] Weinreich, G. and Caussé, R. (1986). Digital and analog bows: hybrid mechanical-electrical systems. In *ICASSP'86. IEEE International Conference on Acoustics, Speech, and Signal Processing*, volume 11, pages 1297–1299. IEEE.

[18] Leroy, N., Fléty, E., and Bevilacqua, F. (2006). Reflective Optical Pickup For Violin. In *International Conference on New Interfaces for Musical Expression (NIME06)*.

[19] Heet, G. S. (1978). String instrument vibration initiator and sustainer. US Patent 4,075,921.

[20] Berdahl, E., Backer, S., and Smith III, J. O. (2005). If I had a Hammer: Design and Theory of an Electromagnetically-prepared Piano. In *Proceedings of the International Computer Music Conference*.

[21] Donovan, L. (2018). *Travelling Wave Control of Stringed Musical Instruments*. PhD thesis, Queen Mary University of London.

[22] Berdahl, E., Smith III, J. O., and Niemeyer, G. (2012). Feedback control of acoustic musical instruments: Collocated control using physical analogs. *The Journal of the Acoustical Society of America*, 131(1):963–973.

[23] Berdahl, E., Smith III, J. O., and Freed, A. (2006). Active damping of a vibrating string. In *2006 International Symposium on Active Control of Sound and Vibration*.

[24] Cheekati, B. and Bhikkaji, B. (2013). A negative imaginary approach to the actuation of a guitar string. *Mechatronics*, 23(8):997–1004.

[25] Boutin, H. and Besnainou, C. (2008). Physical parameters of the violin bridge changed by active control. In *Acoustics'08, Paris*, pages 7247–7252.

[26] Benacchio, S. (2014). *Contrôle actif modal appliqué aux instruments de musique à cordes*. PhD thesis, Université Pierre et Marie Curie – Paris VI.

[27] McPherson, A. (2010). The Magnetic Resonator Piano: Electronic Augmentation of an Acoustic Grand Piano. *Journal of New Music Research*, 39(3):189–202.

[28] HyVibe (2017). Smart Acoustic Guitar, Paris. `https://www.hyvibeguitar.com/`.

[29] Kirchhoff, G. (1876). *Vorlesungen über mathematische Physik: Mechanik*. B. G. Teubner, Leipzig.

[30] Carrier, G. F. (1945). On the non-linear vibration problem of the elastic string. *Quarterly of applied mathematics*, 3(2):157–165.

[31] Chaigne, A. and Kergomard, J. (2016). *Acoustics of musical instruments*. Springer.

[32] Bilbao, S. (2009). *Numerical sound synthesis: finite difference schemes and simulation in musical acoustics*. John Wiley & Sons.

[33] Maschke, B. M. and van der Schaft, A. J. (1992). Port-controlled Hamiltonian systems: modelling origins and systemtheoretic properties. *IFAC Proc. Volumes*, 25(13):359–365.

[34] Curtain, R. F. and Zwart, H. (1995). *An Introduction to Infinite-Dimensional Linear Systems Theory*. Springer.

[35] Villegas, J. A. (2007). *A Port-Hamiltonian Approach to Distributed Parameter Systems*. PhD thesis, University of Twente.

[36] Lopes, N., Hélie, T., and Falaize, A. (2015). Explicit second-order accurate method for the passive guaranteed simulation of port-Hamiltonian systems. *IFAC-PapersOnLine*, 48(13):223–228.

[37] Wijnand, M., d'Andréa-Novel, B., Hélie, T., and Roze, D. (2018). Contrôle des vibrations d'un oscillateur passif : stabilisation en temps fini et par remodelage d'énergie. In *Congrès Français d'Acoustique*.

[38] Falaize, A. and Hélie, T. (2016). Passive Guaranteed Simulation of Analog Audio Circuits: A Port-Hamiltonian Approach. *Applied Sciences*, 6(10):273.

[39] Ortega, R., van der Schaft, A., Maschke, B., and Escobar, G. (2002). Interconnection and damping assignment passivity-based control of port-controlled Hamiltonian systems. *Automatica*, 38(4):585–596.

[40] Hélie, T. and Roze, D. (2016). Corde non linéaire amortie : formulation hamiltonienne à ports, réduction d'ordre exacte et simulation à passivité garantie. In *13ème Congrès Français d'Acoustique*.

[41] Haimo, V. T. (1986). Finite time controllers. *SIAM Journal on Control and Optimization*, 24(4):760–770.

[42] Bhat, S. P. and Bernstein, D. S. (2000). Finite-time stability of continuous autonomous systems. *SIAM Journal on Control and Optimization*, 38(3):751–766.

[43] Bernuau, E., Perruquetti, W., Efimov, D., and Moulay, E. (2015). Robust finite-time output feedback stabilisation of the double integrator. *International Journal of Control*, 88(3):451–460.

[44] Canudas de Wit, C., Siciliano, B., and Bastin, G. (1996). *Theory of Robot Control*. Springer-Verlag.

[45] Hélie, T. and Roze, D. (2008). Sound synthesis of a nonlinear string using Volterra series. *Journal of Sound and Vibration*, 314(1-2):275–306.

[46] Moré, J. J., Garbow, B. S., and Hillstrom, K. E. (1980). User guide for MINPACK-1. Technical report, Argonne National Laboratory.